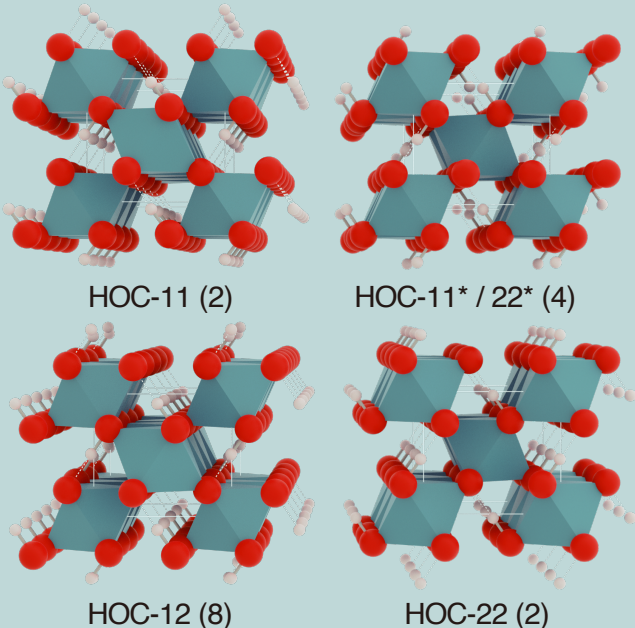
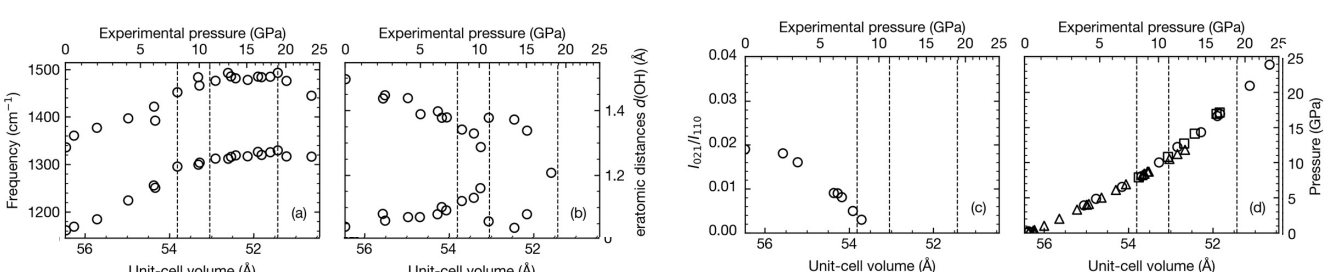


# Ab initio investigation of H-bond disordering in $\delta$ -AlOOH



The H-bond disordering in  $\delta$  was modeled with  $1 \times 1 \times 2$  supercells. Disorder is limited to 1D ( $z$ ) and H-bond arrangements in ( $x, y$ ) was restricted by “ice-rule”-like rules.



$\delta$ -AlOOH is an important hydrous phase that carries water into lower mantle via slab subduction. H-bonds ( $O-H\cdots O$ ) in  $\delta$  is asymmetric at lower pressure. They undergoes symmetrization under compression and become degenerate ionic bonds ( $O-H-O$ ) after the process.

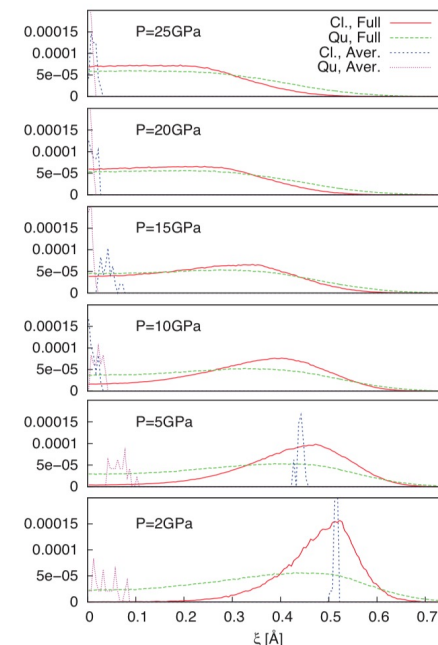
H-bonds in  $\delta$  are localized and independent from the Al-O-Al network which determine the structure.  $\delta$  is an ideal example to study disordering and tunneling, the two process usually associates with the symmetrization because of the reduced energy barrier that facilitates the redistribution of protons.

## Acknowledgement

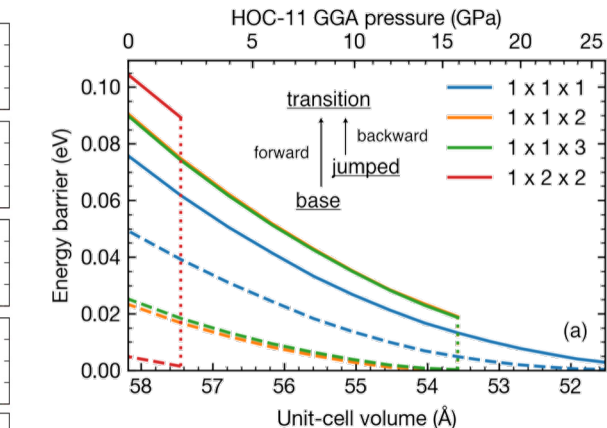
Research supported by DOE grant DE-SC0019759.

## Energy barrier

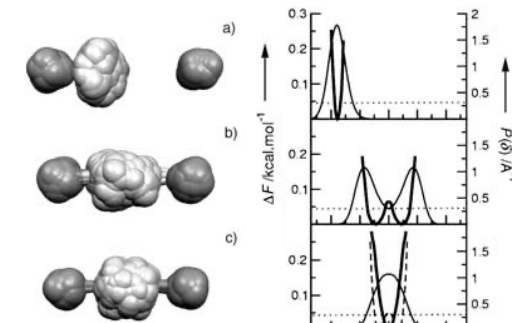
The energy barrier for a single proton jump from nudged-elastic band (NEB) calculation show barrier decreases vs. pressure before full symmetrization. Compared to  $k_B T$  [4] at 300 K, shows tunneling could take place at ~10 GPa, agrees with MD simulation by Bronstein et al. [5].



Proton distribution from MD shows disordering at  $P > 10$  GPa [5].



Energy barrier vs. pressure / volume.

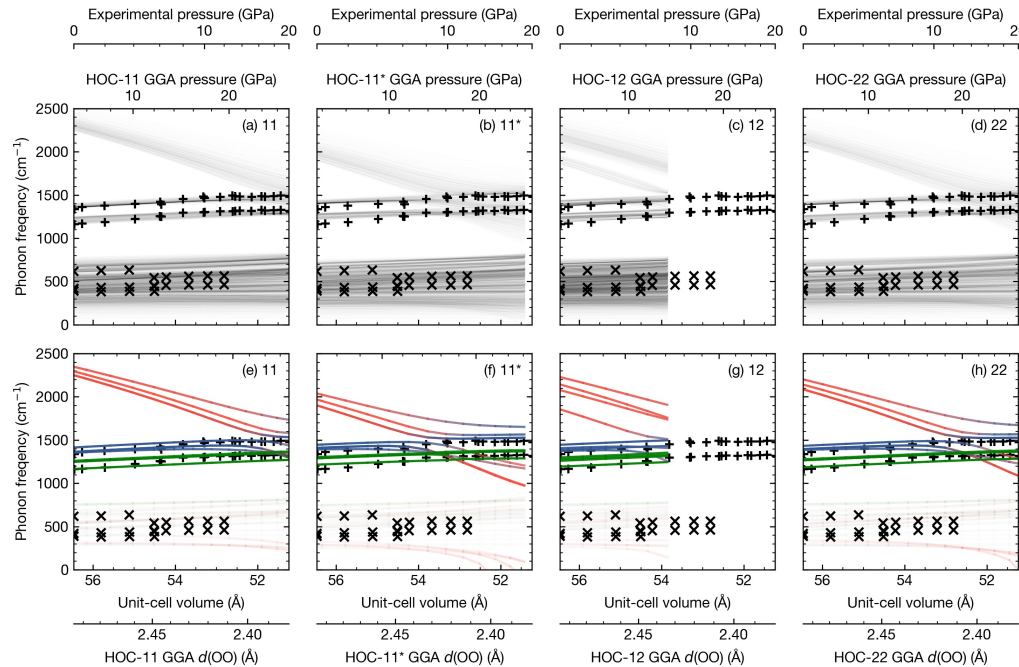


H-bond disordering roughly estimated by comparing energy barrier to  $k_B T$  for ice [4].

1. H. Kagi *et al.*, *J. Phys.: Conf. Ser.* **215**, 012052 (2010).
2. A. Sano-Furukawa *et al.*, *Scientific Reports*. **8**, 15520 (2018).
3. A. Sano-Furukawa *et al.*, *American Mineralogist*. **94**, 1255–1261 (2009).
4. M. Benoit, D. Marx, *ChemPhysChem*. **6**, 1738–1741 (2005).
5. Y. Bronstein, P. Depondt, F. Finocchi, *ejm*. **29**, 385–395 (2017).

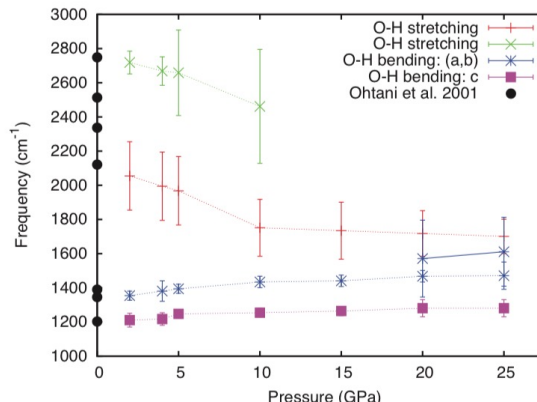
Experimental evidences related to the 300 K multistage transition: (a) IR peaks [1] (b) OH-bond lengths [2] (c) neutron diffraction 021 peak intensity [2] (d) compression curve [3]

# Phonon properties



(a-d) Phonon VDoS vs. pressure; (e-h) : $\Gamma$ -point OH stretching (red), in-plane bending (blue) and out-of-plane bending (green). Higher frequency band corresponds to H-aligned in z; lower frequency band corresponds to H-not aligned.

Phonon modes vs. pressure from supercell MD [1]. Two OH-stretching modes observed in MD at 0-10 GPa; one observed after 10 GPa. Disappearance of high-frequency mode corresponds to disappearance of H-aligned (HOC-11, 22) configuration.



# Thermodynamic properties

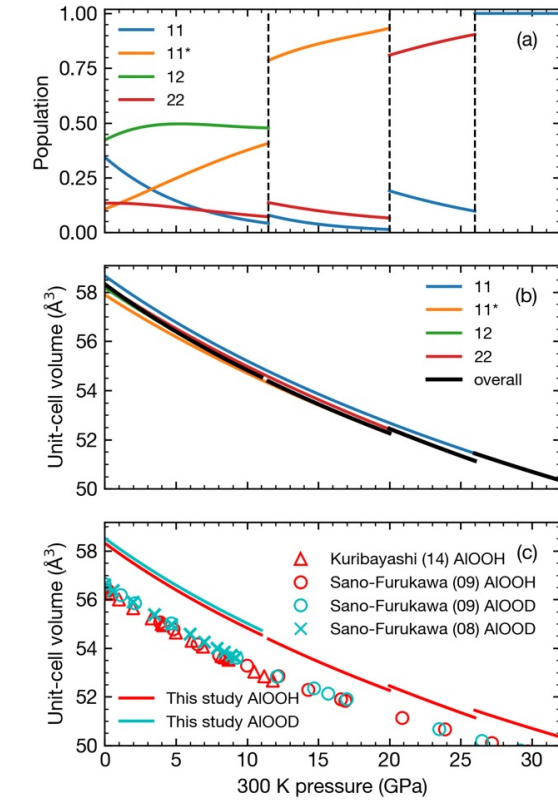
We perform a multiconfiguration QHA to calculate thermodynamic properties of  $\delta$ . The compression curve from mc-QHA shows that disordering explains well the greater compressibility at ~0-8 GPa.

## mc-QHA formalism

$$n_m(V, T) = \frac{Z_m}{Z_{\text{QHA}}} = \frac{g_m \exp \left[ -\frac{F_m(V, T)}{kT} \right]}{\sum_m g_m \exp \left[ -\frac{F_m(V, T)}{kT} \right]}$$

$$F_{\text{QHA}}(V, T) = k_B T \ln Z_{\text{QHA}}(V, T)$$

(a) Pressure evolution of HOC-11, 11\*, 12, and 22 population from mc-QHA at 300 K. (b) Comparison between HOC-11, 11\*, 12, and 22 EoS and the multi-configuration overall EoS; (c) Comparison of  $\delta$ -AlOOH (red) and  $\delta$ -AlOOD (blue) at 300 K. Curve represent overall EoS from mc-QHA.



# Neutron diffraction intensity & bond length

